Quantitative Proteomic Analysis Reveals Metabolic Alterations, Calcium Dysregulation, and Increased Expression of Extracellular Matrix Proteins in Laminin α2 Chain–deficient Muscle*[S]

Bruno Menezes de Oliveira‡§, Cintia Y. Matsumura‡§¶, Cibely C. Fontes-Oliveira§, Kinga I. Gawlik§, Helena Acosta‖, Patrik Wernhoff§, and Madeleine Durbeej§**

Congenital muscular dystrophy with laminin α2 chain deficiency (MDC1A) is one of the most severe forms of muscular disease and is characterized by severe muscle weakness and delayed motor milestones. The genetic basis of MDC1A is well known, yet the secondary mechanisms ultimately leading to muscle degeneration and subsequent connective tissue infiltration are not fully understood. In order to obtain new insights into the molecular mechanisms underlying MDC1A, we performed a comparative proteomic analysis of affected muscles (diaphragm and gastrocnemius) from laminin α2 chain–deficient *dy^{3K}/dy^{3K}* mice, using multidimensional protein identification technology combined with tandem mass tags. Out of the approximately 700 identified proteins, 113 and 101 proteins, respectively, were differentially expressed in the diseased gastrocnemius and diaphragm muscles compared with normal muscles. A large portion of these proteins are involved in different metabolic processes, bind calcium, or are expressed in the extracellular matrix. Our findings suggest that metabolic alterations and calcium dysregulation could be novel mechanisms that underlie MDC1A and might be targets that should be explored for therapy. Also, detailed knowledge of the composition of fibrotic tissue, rich in extracellular matrix proteins, in laminin α2 chain–deficient muscle might help in the design of future anti-fibrotic treatments. All MS data have been deposited in the ProteomeXchange with identifier PXD000978 (http://proteomecentral.proteomexchange.org/dataset/PXD000978). ***Molecular & Cellular Proteomics 13: 10.1074/mcp.M113.032276, 3001–3013, 2014.***

From the §Department of Experimental Medical Science, Unit of Muscle Biology, Lund University, BMC B12, 221 84 Lund, Sweden; ¶Departament of Functional and Structural Biology, Institute of Biology, State University of Campinas (UNICAMP), Campinas, São Paulo 13083-970, Brazil; ‖Stem Cell Center, Lund University, BMC B12, 221 84 Lund, Sweden

Received July 3, 2013, and in revised form, June 26, 2014
Published, MCP Papers in Press, July 3, 2014, DOI 10.1074/mcp.M113.032276
Author contributions: B.M. and M.D. designed research; B.M., C.Y.M., C.C.F., K.I.G., and H.A. performed research; B.M., P.W., and M.D. analyzed data; B.M. and M.D. wrote the paper.

Congenital muscular dystrophy with laminin α2 chain deficiency, also known as MDC1A,[1] is a severe muscle wasting disease for which there is no cure. MDC1A is caused by mutations in the *LAMA2* gene that lead to complete or partial deficiency of laminin α2 chain (1–3). Although the primary defect in MDC1A is known, the secondary molecular mechanisms eventually leading to muscle degeneration are not fully understood. In normal muscle, laminin α2 chain binds to the cell surface receptors dystroglycan and integrin α7β1, which both indirectly bind the cytoskeleton (4–7). Both of these adhesion complexes are important for normal skeletal muscle function, and laminin α2 chain binding to dystroglycan contributes to the maintenance of sarcolemmal integrity and protects muscles from damage (8), whereas laminin α2 chain binding to integrin α7β1 promotes myofiber survival (9, 10). In MDC1A, laminin α2 chain is absent or severely reduced, and the expression of dystroglycan and α7β1 is also dysregulated in MDC1A (9, 11, 12). Thus, the structural link is broken, and the yet to be determined downstream intracellular signaling pathways are also interrupted. Consequently, laminin α2 chain–deficient muscle fibers undergo degeneration–regeneration cycles, but rather quickly regeneration fails and muscle fibers die by apoptosis/necrosis followed by a major replacement of muscle tissue with connective tissue (3, 7). In order to unravel novel secondary molecular mechanisms, which could indicate new therapeutic targets, we decided to evaluate the protein expression profile in laminin α2 chain–deficient *dy^{3K}/dy^{3K}* muscle. Several proteomic profiling studies of dystrophin-deficient muscles (Duchenne muscular dystrophy) have been performed (13–20), as well as some with dysferlin-deficient muscles (Limb-girdle muscular dystrophy type 2B, Miyoshi myopathy) (21, 22). They all showed a great number of proteins that were differentially expressed in different dystrophic muscles and at different ages (13–22). However, proteomic analyses of laminin α2 chain–deficient muscle have not yet been performed. We here used multidimensional protein identification technology with tandem mass tags (TMT), a powerful

[1] The abbreviations used are: MDC1A, merosin congenital muscular dystrophy type 1A; TMT, tandem mass tags.

TABLE I
Experimental setup for gastrocnemius (GAST) and diaphragm (DIA) muscles under two conditions (dy^{3K}/dy^{3K} and wild-type (WT)) and with three biological replicates (pools 1, 2, and 3). The internal standard was a mixture of all samples

	Groups	TMT label
Pool 1 (n=5)	GAST WT	127
	DIA WT	128
	GAST dy^{3K}/dy^{3K}	129
	DIA dy^{3K}/dy^{3K}	130
	Internal standard	126
Pool 2 (n=5)	GAST WT	130
	DIA WT	129
	GAST dy^{3K}/dy^{3K}	128
	DIA dy^{3K}/dy^{3K}	127
	Internal standard	126
Pool 3 (n=5)	GAST WT	129
	DIA WT	130
	GAST dy^{3K}/dy^{3K}	127
	DIA dy^{3K}/dy^{3K}	128
	Internal standard	126

shotgun label-based proteomic method that separates peptides in two-dimensional liquid chromatography (23, 24). We identified around 100 proteins that were differentially expressed in laminin α2 chain–deficient gastrocnemius and diaphragm muscles relative to the corresponding wild-type muscles, and the differential expression of selected proteins was verified with Western blot analysis or immunofluorescence.

EXPERIMENTAL PROCEDURES

Animals—Four-week-old laminin α2 chain–deficient dy^{3K}/dy^{3K} mice and wild-type littermates (n = 15 each) were used (25). Mice were maintained in the animal facilities of BMC (Lund) according to the animal care guidelines. All mouse experimentation was approved by the Malmö/Lund (Sweden) ethical committee for animal research (permit number M62-09).

Protein Extraction, Digestion, TMT Labeling, and Strong Cation Exchange Fractionation—Animals were sacrificed by means of cervical dislocation, and the diaphragm and gastrocnemius muscles were collected, frozen in liquid nitrogen, and pulverized using a mortar and pestle. Subsequently, we used the same experimental setup as previously described (18). Three different pools for each group (dy^{3K}/dy^{3K} and wild-type mice) were made, each composed of muscles from five animals (Table I). Protein was extracted in lysis buffer (10 mM $NaHCO_3$, 5% SDS containing freshly added protease and phosphatase inhibitors (Roche)) via ultrasonication (3 × 5 s at 4 °C). Samples were centrifuged for 5 min (15,000 × g), and supernatant was collected. The protein concentration was determined using a BCA Protein Assay Kit (Pierce). Subsequently, samples were processed according to the instructions for the TMT isobaric mass tagging kits and reagents (Pierce). Briefly, 100 μg of proteins per condition were placed in an Eppendorf tube. Forty-five microliters of 100 mM triethyl ammonium bicarbonate were added to the sample, and the sample was adjusted to a final volume of 100 μl with ultrapure water. Five microliters of 200 mM TCEP (reducing agent) were added and incubated at 55 °C for 1 h. Five microliters of 375 mM iodoacetamide was added, and samples were incubated for 30 min while protected from light. After this, samples were precipitated overnight with six volumes of prechilled (−20 °C) acetone. Finally, protein pellets were resuspended in 100 μl of 100 mM triethyl ammonium bicarbonate. At this point trypsin was added, and proteolytic digestion was allowed overnight at 37 °C. Label reagents were prepared at room temperature, and 41 μl of each reagent were used to label 100 μg of protein. Besides our four samples to be analyzed, a standard one, composed of equal fractions of the four others, was labeled. This standard sample was our reference, used to define the relative protein amounts for each analyzed sample. Our labeling design allowed a label swap, in order to avoid possible bias due to technical errors (Table I). The label reaction proceeded for 1 h at room temperature, and subsequently reactions were quenched with 8 μl of 5% hydroxylamine for 15 min, mixed, and stored at −80 °C. Pooled TMT-labeled samples were fractionated by strong cation exchange (Applied Biosystems, Foster City, CA) using 500 μl of elution buffer (KH_2PO_4, 25 mM acetonitrile, pH 2.9) containing increasing concentrations of KCl (30, 60, 90, 120, 240, 300, 420, and 500 mM KCl) and collected as fractions 1–8, respectively. The fractions were cleaned on Ultra Microspin C18 columns (The Nest Group, Southborough, MA), dried, and resuspended in 30 μl of 0.1% formic acid.

LC-MS/MS Analysis on LTQ-OrbitrapXL—Samples were analyzed at the Gothenburg Proteomics Core, Gothenburg University, following the protocol described below. Desalted and dried fractions were reconstituted into 0.1% formic acid and analyzed on an LTQ-OrbitrapXL (Thermo Fisher Scientific) interfaced with an in-house-constructed nano-LC column. Two-microliter sample injections were made with an HTC-PAL autosampler (CTC Analytics AG, Zwingen, Switzerland) connected to an Agilent 1200 binary pump (Agilent Technologies, Santa Clara, CA). The peptides were trapped on a precolumn (40 × 0.075 mm inner diameter) and separated on a reversed phase column (200 × 0.050 mm). Both columns were packed in-house with 3-μm Reprosil-Pur C18-AQ particles. The flow through the analytical column was reduced by a split to ~100 nl/min, and the gradient was as follows; 0–6 min, 0.1% formic acid; 6–76 min, 7% to 35% acetonitrile, 0.1% formic acid; 76–79 min, 40% to 80% acetonitrile, 0.1% formic acid. LTQ-OrbitrapXL settings were as follows: spray voltage, 1.4 kV; 1 microscan for MS1 scans at 60,000 resolution (m/z 400); full MS mass range, m/z 400–2000. The LTQ-OrbitrapXL was operated in a data-dependent mode with one MS1 Fourier transform MS scan of precursor ions followed by collision-induced dissociation and high-energy collision dissociation MS2 scans of the three most abundant doubly, triply, and quadruply protonated ions in each Fourier transform MS scan. The settings for the MS2 were as follows: 1 microscan for high-energy collision dissociation MS2 at 7500 resolution (at m/z 400), mass range of m/z 100–2000 with a collision energy of 50%, and 1 microscan for collision-induced dissociation MS2 with a collision energy of 30%. Dynamic exclusion of a precursor selected for MS2 was used for 120 s after one repeat, allowing most of the co-eluting precursors to be selected for MS2. All samples were analyzed a second time as described above, and also a third time using an exclusion list of all m/z within a 3-min retention window, already passing the identification criteria within the TMT set (eight fractions) in the database search.

Database Search and TMT Quantification—MS raw data files from all eight strong cation exchange fractions per one TMT set and three MS runs were merged for relative quantification and identification using Proteome Discoverer version 1.3 (Thermo Fisher Scientific). The database search was performed with the Mascot search engine using the following criteria: *Mus musculus* in Swiss-Prot protein database from April 2012 (535,698 entries); MS peptide tolerance of 10 ppm; MS/MS tolerance of 0.5 Da; trypsin digestion allowing one missed

cleavage with variable modifications (methionine oxidation, cysteine methylthiol) and fixed modifications (N-terminal TMT6-plex label, lysine TMT6-plex label). The detected protein threshold in the software was set to a confidence using the 1% false discovery rate method, and identified proteins were grouped by shared sequence to minimize redundancy. For quantification, the ratios of TMT reporter ion intensities in MS/MS spectra (*m/z* 126.12, 127.13, 128.13, 129.14, 130.14) from raw datasets were used to calculate fold changes between samples via the relative ratio to the reference pool. Only peptides unique for a given protein were considered for relative quantitation, excluding those common to other isoforms or proteins of the same family. Only peptides with a score of >10 and below the Mascot significance threshold filter of $p = 0.05$ were included. Single peptide identifications required a score equal to or above the Mascot identity threshold. Normalization of protein median was used, and the median of peptides was used for determining protein ratio; the resulting ratios were exported into Excel for manual data interpretation. The mass spectrometry proteomics data have been deposited to the ProteomeXchange Consortium (http://proteomecentral.proteomexchange.org) via the PRIDE partner repository (26) with the dataset identifier PXD000978. Please see the supplemental material for annotated spectra and Table I for the experimental setup.

Data Analysis—To determine which proteins were differentially expressed, only proteins quantified in all three runs (see Table I for the experimental setup) were used; average values were compared, and Student's *t* test was performed to validate differences ($p < 0.05$) (supplemental Tables S1–S3). Still, compared proteins should present a variation coefficient of less than 25% and a protein ratio less than 1.25 or greater than 1.25. In order to avoid multiple hypothesis test error, *q*-values were estimated (27, 28). Also, to ensure the reproducibility of our findings, the retrospective statistical power was calculated using the free statistical software package R, according to Ref. 29. Only results for $\beta \geq 0.8$ were validated as true.

Western Blot Analysis—Muscles were collected and proteins were extracted as described above, but from a different animal cohort ($n = 4$ for each genotype). Thirty micrograms of total protein were applied per well. SDS-PAGE was performed according to Laemmli's protocol using 12% pre-casted gels in a Mini Protean Tetracell Electrophoresis System (Bio-Rad), followed by electrophoretic transfer. PVDF membranes were blocked in 5% non-fat dry milk in TBS with 0.05% Tween-20 overnight at 4 °C. Membranes were incubated with primary antibodies (rabbit anti-isocitrate dehydrogenase, 1:1000, NBP1–31599, Novus (Littleton, CO); mouse anti-SERCA1 ATPase, 1:4000, ab2819, Abcam; mouse anti-calsequestrin 1 and 2, 1:1000, ab3516, Abcam (Cambridge, UK); goat anti-annexin A1, 1:1000, NBP1–18842) for 1 h at room temperature and subsequently washed three times for 10 min in TBS with 5% Tween-20. Membranes were once again blocked in 5% non-fat dry milk for 1 h and then incubated with secondary antibodies (1 h at room temperature). After three 10-min washes with TBS with 5% Tween-20, membranes were incubated in ECL chemiluminiscence solution (Amersham Biosciences), exposed to Hyperfilm (Amersham Biosciences), and developed (Curix 60, AGFA, Mortsel, Belgium). We applied the Mann–Whitney *U* test to assess whether the difference in protein expression was statistically significant. Statistical significance was accepted for $p < 0.05$.

Immunofluorescence—Skeletal muscle (quadriceps and diaphragm) sections of 7 μm were processed for immunofluorescence analyses following standard procedures (30) with rabbit polyclonal antibodies directed against periostin (1:200, NBP1–30042, Novus) and galectin-1 (1:100, NBP1–89791, Novus). Sections were analyzed using a Zeiss Axioplan fluorescence microscope. Images were captured using an ORCA 1394 ER digital camera with the Openlab 3 software.

RESULTS

Shotgun Proteomic Analysis of Laminin α2 Chain–deficient Gastrocnemius and Diaphragm—Two-dimensional polyacrylamide gel electrophoresis has mainly been used as the proteomic approach to analyze dystrophic muscle (13–17). To overcome several drawbacks associated with this technique, we decided to use a label-based proteomic approach combining TMT labels and the multidimensional protein identification technology method. In this kind of analysis, whole samples are digested with a protease prior to identification and quantification of proteins in the sample. In our case we used trypsin, and peptides were labeled with an isobaric tag (TMT) for quantification (24). Subsequently, samples were fractionated using biphasic capillary columns packed with strong cation exchange and reversed phase material to separate digested and TMT-labeled whole protein mixtures. Labeled peptides were thus separated based on their charge and hydrophobicity, and the identification and quantification of peptides in eluted fractions was achieved using a mass spectrometer (peptides were identified through database searching and quantified by evaluation of reporter ion intensities from labels) (31, 32).

We analyzed gastrocnemius and diaphragm muscles from 4-week-old laminin α2 chain–deficient dy^{3K}/dy^{3K} and age-matched wild-type littermates. At this age, dy^{3K}/dy^{3K} muscles display typical pathological hallmarks such as small or rounded fibers (which indicate de-/regeneration), variation in muscle fiber diameter, centralized nuclei (indicative of regeneration), and the presence of inflammatory cells or adipose and fibrotic tissue (25, 33). With the multidimensional protein identification technology approach, we identified around 700 proteins in gastrocnemius and diaphragm muscles (supplemetal Table S4). Among these, 113 and 101 proteins, respectively, were found to be differentially altered in their levels by at least a factor of ±1.25 in dy^{3K}/dy^{3K} gastrocnemius and diaphragm muscle relative to corresponding wild-type muscles. In laminin α2 chain–deficient gastrocnemius muscle, there were 82 down-regulated and 31 up-regulated proteins, and in diaphragm muscle, 77 proteins were down-regulated and 24 were up-regulated. Around 62% of the down-regulated proteins and ~67% of the up-regulated proteins in the two muscles were identical (Tables II–V). Overall, a vast majority of the differentially expressed proteins were intracellular proteins, but also several extracellular and plasma membrane proteins were identified. We used the PANTHER classification system to group the proteins with differential expression into different biological processes. Among the down-regulated proteins were proteins involved in metabolic processes, generation of precursor metabolites and energy, cellular processes, system processes, transport processes, and developmental processes. Among the up-regulated proteins were proteins involved in cellular processes, metabolic processes, cellular component organiza-

TABLE II
Underrepresented proteins in laminin α2 chain–deficient gastrocnemius versus wild-type gastrocnemius

Accession	Description	Σ Coverage	*p* value	Σ Number of peptides	Fold change
P32848	Parvalbumin α	66.36	6.13E-01	11	−3.59
O88990	α-Actinin-3	45.33	7.11E-01	33	−2.98
Q5XKE0	Myosin-binding protein C, fast-type	33.19	9.80E-01	32	−2.97
Q5SX39	Myosin-4	61.84	9.50E-01	140	−2.96
Q3TJD7	PDZ and LIM domain protein 7	4.16	8.09E-01	2	−2.65
P07310	Creatine kinase M-type	61.42	4.90E-01	25	−2.56
P05064	Fructose-bisphosphate aldolase A	43.96	8.75E-01	18	−2.40
Q9WUB3	Glycogen phosphorylase, muscle form	42.87	9.41E-01	35	−2.35
O70250	Phosphoglycerate mutase 2	34.39	7.39E-01	9	−2.33
P58771	Tropomyosin α-1 chain	74.30	6.96E-01	31	−2.21
P21550	β-Enolase	40.09	8.30E-01	18	−2.10
Q9D6R2	Isocitrate dehydrogenase [NAD] subunit α, mitochondrial	11.20	5.59E-01	3	−2.06
P06151	L-lactate dehydrogenase A chain	37.35	7.17E-01	16	−2.03
Q8R429	Sarcoplasmic/endoplasmic reticulum calcium ATPase 1	32.39	6.11E-01	34	−2.01
Q9QZ47	Troponin T, fast skeletal muscle	30.15	5.16E-01	9	−2.00
P13707	Glycerol-3-phosphate dehydrogenase [NAD+], cytoplasmic	25.50	9.96E-01	7	−1.97
P47857	6-phosphofructokinase, muscle type	22.69	7.64E-01	14	−1.93
O08532	Voltage-dependent calcium channel subunit α-2/δ-1	3.81	5.37E-01	2	−1.92
P13412	Troponin I, fast skeletal muscle	28.57	7.49E-01	6	−1.89
P17751	Triosephosphate isomerase	34.78	7.51E-01	8	−1.89
P20801	Troponin C, skeletal muscle	47.50	6.61E-01	6	−1.89
P28650	Adenylosuccinate synthetase isozyme 1	17.94	7.11E-01	6	−1.89
P09411	Phosphoglycerate kinase 1	27.34	9.91E-01	11	−1.89
Q9D0F9	Phosphoglucomutase-1	15.48	9.27E-01	8	−1.89
O09165	Calsequestrin-1	23.21	7.28E-01	10	−1.87
P16858	Glyceraldehyde-3-phosphate dehydrogenase	46.25	8.51E-01	12	−1.84
Q9R0Y5	Adenylate kinase isoenzyme 1	57.73	6.36E-01	12	−1.82
P62631	Elongation factor 1-α 2	31.97	9.43E-01	11	−1.76
P52480	Pyruvate kinase isozymes M1/M2	36.35	9.38E-01	15	−1.75
P56392	Cytochrome c oxidase subunit 7A1, mitochondrial	16.25	6.95E-01	1	−1.75
Q9JK37	Myozenin-1	39.19	6.91E-01	8	−1.72
Q6P8J7	Creatine kinase S-type, mitochondrial	33.65	5.68E-01	14	−1.72
Q60932	Voltage-dependent anion-selective channel protein 1	47.97	6.69E-01	11	−1.71
P06745	Glucose-6-phosphate isomerase	17.38	8.76E-01	9	−1.71
Q91YE8	Synaptopodin-2	2.58	6.30E-01	3	−1.70
A2ASS6	Titin	19.75	6.91E-01	550	−1.70
P63038	60 kDa heat shock protein, mitochondrial	17.63	7.56E-01	9	−1.68
Q9CR68	Cytochrome b-c1 complex subunit Rieske, mitochondrial	46.35	5.81E-01	7	−1.67
Q9WUM5	Succinyl-CoA ligase [GDP-forming] subunit α, mitochondrial	14.74	4.92E-01	5	−1.67
Q9D855	Cytochrome b-c1 complex subunit 7	20.72	6.22E-01	2	−1.66
P97457	Myosin regulatory light chain 2, skeletal muscle isoform	71.60	9.22E-01	16	−1.66
P05977	Myosin light chain 1/3, skeletal muscle isoform	76.06	8.05E-01	18	−1.66
P68134	Actin, α skeletal muscle	58.62	5.40E-01	23	−1.66
P08249	Malate dehydrogenase, mitochondrial	46.45	4.87E-01	13	−1.65
Q61425	Hydroxyacyl-coenzyme A dehydrogenase, mitochondrial	17.83	5.72E-01	4	−1.63
Q9CQC7	NADH dehydrogenase [ubiquinone] 1 β subcomplex subunit 4	27.13	6.62E-01	2	−1.59
Q62234	Myomesin-1	16.08	6.80E-01	22	−1.59
Q06185	ATP synthase subunit e, mitochondrial	35.21	7.80E-01	2	−1.59
Q9Z1E4	Glycogen [starch] synthase, muscle	1.08	5.65E-01	1	−1.59
P14152	Malate dehydrogenase, cytoplasmic	25.75	6.77E-01	6	−1.56
Q9Z2I9	Succinyl-CoA ligase [ADP-forming] subunit β, mitochondrial	11.23	6.86E-01	6	−1.53
Q9D051	Pyruvate dehydrogenase E1 component subunit β, mitochondrial	29.53	6.87E-01	8	−1.53
Q9D3D9	ATP synthase subunit δ, mitochondrial	41.07	4.95E-01	4	−1.52
O08749	Dihydrolipoyl dehydrogenase, mitochondrial	14.93	6.08E-01	5	−1.51
Q9CPQ1	Cytochrome c oxidase subunit 6C	21.05	9.04E-01	2	−1.50
P01942	Hemoglobin subunit α	71.13	7.73E-01	9	−1.50
Q99KI0	Aconitate hydratase, mitochondrial	31.79	4.90E-01	21	−1.49
P58774	Tropomyosin β chain	79.23	5.15E-01	34	−1.48
P12787	Cytochrome c oxidase subunit 5A, mitochondrial	39.04	6.12E-01	8	−1.48

TABLE II—*continued*

Accession	Description	Σ Coverage	*p* value	Σ Number of peptides	Fold change
Q9CZU6	Citrate synthase, mitochondrial	34.70	5.37E-01	11	−1.46
Q9DCX2	ATP synthase subunit d, mitochondrial	69.57	9.78E-01	9	−1.45
P54071	Isocitrate dehydrogenase [NADP], mitochondrial	28.32	6.62E-01	11	−1.45
Q9DCW4	Electron transfer flavoprotein subunit β	42.35	6.38E-01	11	−1.44
Q8VEM8	Phosphate carrier protein, mitochondrial	14.57	6.39E-01	6	−1.44
P56480	ATP synthase subunit β, mitochondrial	64.46	5.28E-01	22	−1.43
Q91WD5	NADH dehydrogenase [ubiquinone] iron-sulfur protein 2, mitochondrial	12.31	6.08E-01	4	−1.43
Q9JKS4	LIM domain-binding protein 3	17.01	5.78E-01	9	−1.42
P19783	Cytochrome c oxidase subunit 4 isoform 1, mitochondrial	20.71	7.65E-01	5	−1.41
Q07417	Short-chain specific acyl-CoA dehydrogenase, mitochondrial	7.77	5.59E-01	3	−1.40
P56391	Cytochrome c oxidase subunit 6B1	20.93	5.00E-01	3	−1.40
Q9DB20	ATP synthase subunit O, mitochondrial	41.31	4.98E-01	9	−1.39
P35486	Pyruvate dehydrogenase E1 component subunit α, somatic form, mitochondrial	19.74	9.28E-01	6	−1.39
Q9CZ13	Cytochrome b-c1 complex subunit 1, mitochondrial	19.17	8.11E-01	9	−1.38
P05202	Aspartate aminotransferase, mitochondrial	26.98	6.77E-01	10	−1.37
Q8R1I1	Cytochrome b-c1 complex subunit 9	39.06	5.25E-01	3	−1.37
Q03265	ATP synthase subunit α, mitochondrial	54.97	5.37E-01	27	−1.33
Q91YT0	NADH dehydrogenase [ubiquinone] flavoprotein 1, mitochondrial	19.61	7.55E-01	7	−1.32
Q9D2G2	Dihydrolipoyllysine-residue succinyltransferase component of 2-oxoglutarate dehydrogenase complex, mitochondrial	12.33	5.87E-01	5	−1.31
P70670	Nascent polypeptide-associated complex subunit α, muscle-specific form	1.19	7.92E-01	3	−1.28
P97807	Fumarate hydratase, mitochondrial	25.44	5.55E-01	12	−1.27
Q7TQ48	Sarcalumenin	21.76	7.18E-01	12	−1.27
P11404	Fatty acid–binding protein, heart	54.14	5.67E-01	7	−1.26

tion, cell communication, developmental processes, and system processes (Figs. 1*A*–1*D*). Oxidoreductases, transferases, cytoskeletal proteins, and calcium-binding proteins were among the most underrepresented proteins in dy^{3K}/dy^{3K} muscles, whereas receptors, calcium-binding proteins, cytoskeletal proteins, and extracellular matrix proteins were among the most overrepresented proteins (Tables II–V).

Altered Metabolism in Laminin α2 Chain–deficient Muscle—A clear majority of the down-regulated proteins belonged to the class of metabolic processes/generation of precursor metabolites and energy, such as glycolysis, fatty acid β-oxidation, acyl CoA metabolic processes, pyrimidine and purin base metabolic processes, tricarboxylic acid cycle, oxidative phosphorylation, and respiratory electron transport chain (Tables II and IV). Each of these pathways is complex, involving numerous proteins. For example, the following proteins were down-regulated in laminin α2 chain–deficient muscles: fructose-biphosphate aldolase A, 6-phosphofrucokinase, L-lactate dehydrogenase, and glucose-6-phosphate isomerase (glycolysis-related); short-chain specific acyl-CoA dehydrogenase, medium-chain specific acyl-CoA dehydrogenase, and 2,4-dienoyl-CoA reductase (involved in fatty acid β-oxidation and acyl coA metabolic processes); adenylate kinase isoenzyme 1, phosphoglutamase-1, and various subunits of ATP synthase (pyrimidine and purin base metabolic processes); isocitrate dehydrogenase, succinyl-CoA ligase, malate dehydrogenase, and citrate synthase (tricarboxylic acid cycle–related); and various subunits of cytochrome *c* oxidase, electron transfer flavoprotein, and various subunits of ATP synthase (involved in oxidative phosphorylation and respiratory electron transport chain). Also, in a previous gene expression profiling study we noted that several down-regulated genes were assigned to metabolic themes (34). We next performed Western blot analysis to validate the proteomic findings, and indeed isocitrate dehydrogenase was significantly down-regulated in laminin α2 chain–deficient muscle (Fig. 2).

Impaired Calcium Homeostasis in Laminin α2 Chain–deficient Muscle—An increase in cytosolic calcium concentration has been connected to the pathomechanism of muscular dystrophy (35), but it is not yet clear whether impaired calcium homeostasis is pathogenic in MDC1A. In some muscular dystrophies (*e.g.* Duchenne muscular dystrophy), the muscle cell membrane is easily damaged, and this could lead to an influx of calcium in the cell; alternatively, enhanced calcium entry may occur through a class of stretch-activated channels. The increased calcium leads to necrosis and/or apoptosis of the muscle fiber through distinct mechanisms (36–38). Also, the expression levels of proteins involved in the regulation of intracellular calcium concentration could be altered in muscular dystrophy (39). In MDC1A, there is little evidence of sarcolemmal disruption (40, 41), but we noted

TABLE III
Overrepresented proteins in laminin α2 chain–deficient gastrocnemius versus wild-type gastrocnemius

Accession	Description	Σ Coverage	*p* value	Σ Number of peptides	Fold change
Q62009	Periostin	4.30	1.96E-05	2	4.95
Q9Z1T2	Thrombospondin-4	3.63	2.84E-02	2	3.75
P10107	Annexin A1	10.40	1.87E-03	3	3.18
P62962	Profilin-1	27.14	4.90E-04	3	2.82
P62806	Histone H4	52.43	1.25E-02	7	2.38
P04117	Fatty acid–binding protein, adipocyte	29.55	8.51E-03	5	2.31
P16045	Galectin-1	17.78	5.24E-04	2	2.27
P20152	Vimentin	53.86	2.25E-02	26	2.20
P51885	Lumican	25.15	1.40E-02	7	2.18
P28653	Biglycan	28.18	1.56E-02	8	2.12
P15864	Histone H1.2	33.02	1.45E-04	9	2.05
P48036	Annexin A5	22.88	7.68E-04	7	1.98
P48678	Prelamin-A/C	26.32	2.03E-03	14	1.97
Q9D0J8	Parathymosin	11.88	1.30E-03	1	1.87
P43276	Histone H1.5	8.97	2.17E-03	2	1.79
P97447	Four and a half LIM domains protein 1	11.07	1.65E-02	3	1.78
O88569	Heterogeneous nuclear ribonucleoproteins A2/B1	9.63	9.16E-03	3	1.75
P10854	Histone H2B type 1-M	47.62	3.04E-03	7	1.73
P13542	Myosin-8	48.89	1.57E-02	111	1.66
P68433	Histone H3.1	16.91	1.34E-02	3	1.64
P23927	α-Crystalline B chain	20.00	2.58E-02	3	1.60
Q8VHX6	Filamin-C	9.98	5.25E-03	18	1.55
Q9CZM2	60S ribosomal protein L15	16.18	1.69E-02	3	1.54
Q8CGP6	Histone H2A type 1-H	32.03	8.67E-03	4	1.53
P17742	Peptidyl-prolyl cis-trans isomerase A	27.44	8.84E-04	5	1.51
P62301	40S ribosomal protein S13	23.18	8.58E-04	3	1.44
Q8BH64	EH domain-containing protein 2	15.47	2.39E-02	6	1.39
Q04857	Collagen α-1(VI) chain	12.20	2.79E-02	11	1.38
O09161	Calsequestrin-2	9.88	2.14E-02	4	1.37
P10922	Histone H1.0	26.80	1.55E-02	5	1.36
P07724	Serum albumin	31.09	1.44E-02	22	1.35

that parvalbumin, a protein that acts as a soluble intracellular calcium buffer (and is present in high concentrations in fast-contracting skeletal muscles), was significantly down-regulated in laminin α2 chain–deficient muscles (Table II and IV, first protein in the lists). Also, SERCA1 (which resides in the sarcoplasmic reticulum and transfers calcium from cytosol to sarcoplasmic reticulum lumen) was down-regulated in laminin α2 chain–deficient muscles, as was calsequestrin-1 (which also resides in sarcoplasmic reticulum and helps hold calcium in sarcoplasmic reticulum) (Tables II and IV; Fig. 2). The expression of calsequestrin-2, in contrast, was up-regulated, at least in gastrocnemius muscle (Table III; Fig. 2).

Inflammation and Composition of Fibrotic Tissue in Laminin α2 Chain–deficient Muscle—We detected increased levels of annexins A1, A2, and A5 in laminin α2 chain–deficient muscle (Tables III and V). The annexins are phospholipid- and calcium-binding proteins involved in numerous physiological processes (42). Several members of the annexin family (*e.g.* annexins A1, A2, and A5) are differentially expressed in normal muscle relative to Duchenne muscular dystrophy, and the three annexins are highly expressed in macrophages and T cells in dystrophin-deficient muscle (18, 43). The annexins could therefore have a role in the inflammatory response in muscular dystrophy, and MDC1A is indeed characterized by early-onset transient inflammation (44).

Furthermore, several of the up-regulated proteins are extracellular matrix proteins. Previous gene expression profiling experiments have demonstrated that up-regulation of genes encoding extracellular matrix components is more pronounced in congenital muscular dystrophies (including MDC1A) than in Duchenne muscular dystrophy (45). Yet the composition and properties of fibrotic lesions in laminin α2 chain–deficient chain muscle have not been extensively studied. The expression of periostin, galectin-1, collagen VI α2 chain, biglycan, lumican, and thrombospondin-4 was significantly increased in laminin α2 chain–deficient skeletal muscles (Tables III and V). Immunostaining of selected proteins (periostin and galectin-1) was performed to validate the proteomics data. Periostin expression was dramatically increased in laminin α2 chain–deficient muscle (Fig. 3), and galectin-1 was moderately augmented (Fig. 3).

TABLE IV
Under-represented proteins in laminin α2 chain deficient-diaphragm versus wild-type diaphragm

Accession	Description	Σ Coverage	*p* value	Σ Number of peptides	Fold change
P32848	Parvalbumin α	66.36	8.62E-03	11	−4.12
P04247	Myoglobin	57.14	6.47E-03	10	−1.99
Q9WUB3	Glycogen phosphorylase, muscle form	42.87	3.09E-03	35	−1.98
P56392	Cytochrome c oxidase subunit 7A1, mitochondrial	16.25	7.82E-03	1	−1.78
Q5SX40	Myosin-1	61.79	7.96E-03	141	−1.71
O09165	Calsequestrin-1	23.21	8.62E-03	10	−1.71
P16125	L-lactate dehydrogenase B chain	25.15	6.29E-04	10	−1.68
P13707	Glycerol-3-phosphate dehydrogenase [NAD+], cytoplasmic	25.50	3.10E-03	7	−1.66
Q9D023	Brain protein 44	22.83	6.95E-03	4	−1.64
P13412	Troponin I, fast skeletal muscle	28.57	8.36E-03	6	−1.64
P16015	Carbonic anhydrase 3	46.92	4.44E-03	10	−1.63
P07310	Creatine kinase M-type	61.42	5.35E-03	25	−1.62
Q9CQC7	NADH dehydrogenase [ubiquinone] 1 β subcomplex subunit 4	27.13	1.04E-02	2	−1.61
Q9R0Y5	Adenylate kinase isoenzyme 1	57.73	4.19E-03	12	−1.59
Q9CXZ1	NADH dehydrogenase [ubiquinone] iron-sulfur protein 4, mitochondrial	8.57	1.86E-02	1	−1.58
Q60932	Voltage-dependent anion-selective channel protein 1	47.97	2.76E-02	11	−1.56
Q8R429	Sarcoplasmic/endoplasmic reticulum calcium ATPase 1	32.39	1.49E-02	34	−1.55
P21550	β-enolase	40.09	1.56E-02	18	−1.54
P45952	Medium-chain specific acyl-CoA dehydrogenase, mitochondrial	19.48	4.87E-04	8	−1.53
Q9DCS9	NADH dehydrogenase [ubiquinone] 1 β subcomplex subunit 10	14.20	1.63E-02	2	−1.53
Q9D6J6	NADH dehydrogenase [ubiquinone] flavoprotein 2, mitochondrial	12.10	4.23E-03	2	−1.53
Q99JY0	Trifunctional enzyme subunit β, mitochondrial	25.26	6.01E-03	11	−1.53
Q924X2	Carnitine O-palmitoyltransferase 1, muscle isoform	9.59	1.34E-02	6	−1.52
P19783	Cytochrome c oxidase subunit 4 isoform 1, mitochondrial	20.71	1.43E-03	5	−1.52
P97457	Myosin regulatory light chain 2, skeletal muscle isoform	71.60	1.63E-02	16	−1.51
Q9Z2I9	Succinyl-CoA ligase [ADP-forming] subunit β, mitochondrial	11.23	1.95E-02	6	−1.50
P41216	Long-chain-fatty-acid–CoA ligase 1	17.31	3.95E-03	11	−1.50
Q6P8J7	Creatine kinase S-type, mitochondrial	33.65	4.52E-03	14	−1.50
P20801	Troponin C, skeletal muscle	47.50	2.44E-02	6	−1.48
Q9DCT2	NADH dehydrogenase [ubiquinone] iron-sulfur protein 3, mitochondrial	20.53	1.07E-02	5	−1.48
P05977	Myosin light chain 1/3, skeletal muscle isoform	76.06	5.77E-03	18	−1.47
Q91VD9	NADH-ubiquinone oxidoreductase 75 kDa subunit, mitochondrial	16.78	2.11E-02	9	−1.47
Q9WUM5	Succinyl-CoA ligase [GDP-forming] subunit α, mitochondrial	14.74	8.82E-03	5	−1.47
P48962	ADP/ATP translocase 1	41.28	1.39E-02	14	−1.47
P05201	Aspartate aminotransferase, cytoplasmic	32.20	5.97E-03	11	−1.47
P28650	Adenylosuccinate synthetase isozyme 1	17.94	2.70E-02	6	−1.46
P62897	Cytochrome c, somatic	50.48	2.11E-03	6	−1.46
P05064	Fructose-bisphosphate aldolase A	43.96	1.17E-02	18	−1.46
P11404	Fatty acid–binding protein, heart	54.14	1.42E-04	7	−1.46
P54071	Isocitrate dehydrogenase [NADP], mitochondrial	28.32	7.79E-03	11	−1.46
Q8BMS1	Trifunctional enzyme subunit α, mitochondrial	41.28	2.86E-02	23	−1.46
Q9CZU6	Citrate synthase, mitochondrial	34.70	3.01E-02	11	−1.45
P08249	Malate dehydrogenase, mitochondrial	46.45	1.70E-03	13	−1.44
Q9QZ47	Troponin T, fast skeletal muscle	30.15	5.33E-03	9	−1.44
Q3TJD7	PDZ and LIM domain protein 7	4.16	5.81E-03	2	−1.44
P12787	Cytochrome c oxidase subunit 5A, mitochondrial	39.04	2.12E-02	8	−1.42
Q9CQ62	2,4-dienoyl-CoA reductase, mitochondrial	28.06	4.55E-03	7	−1.42
Q60936	Chaperone activity of bc1 complex-like, mitochondrial	9.61	6.42E-03	5	−1.42
P97807	Fumarate hydratase, mitochondrial	25.44	2.82E-03	12	−1.42
Q9DCW4	Electron transfer flavoprotein subunit β	42.35	1.05E-02	11	−1.41
Q9CPQ1	Cytochrome c oxidase subunit 6C	21.05	2.78E-02	2	−1.41
P58774	Tropomyosin β chain	79.23	1.19E-02	34	−1.41
P56391	Cytochrome c oxidase subunit 6B1	20.93	4.53E-03	3	−1.40
Q9DCX2	ATP synthase subunit d, mitochondrial	69.57	1.25E-02	9	−1.39
Q91VR2	ATP synthase subunit γ, mitochondrial	25.17	1.51E-02	9	−1.39
Q99LC3	NADH dehydrogenase [ubiquinone] 1 α subcomplex subunit 10, mitochondrial	14.08	1.38E-02	4	−1.39
P56480	ATP synthase subunit β, mitochondrial	64.46	6.68E-03	22	−1.39

TABLE IV—*continued*

Accession	Description	Σ Coverage	*p* value	Σ Number of peptides	Fold change
P14152	Malate dehydrogenase, cytoplasmic	25.75	2.26E-04	6	−1.39
Q60597	2-oxoglutarate dehydrogenase, mitochondrial	12.71	2.77E-02	11	−1.38
Q8CAQ8	Mitochondrial inner membrane protein	15.59	1.73E-02	10	−1.37
Q9D3D9	ATP synthase subunit δ, mitochondrial	41.07	4.05E-03	4	−1.37
P47857	6-phosphofructokinase, muscle type	22.69	1.46E-02	14	−1.36
Q9CQQ7	ATP synthase subunit b, mitochondrial	23.05	5.29E-03	5	−1.36
P58771	Tropomyosin α-1 chain	74.30	1.78E-02	31	−1.36
Q99KI0	Aconitate hydratase, mitochondrial	31.79	1.05E-02	21	−1.35
Q9DB20	ATP synthase subunit O, mitochondrial	41.31	1.26E-02	9	−1.35
Q62234	Myomesin-1	16.08	2.91E-02	22	−1.35
Q9CQ69	Cytochrome b-c1 complex subunit 8	34.15	1.23E-02	3	−1.34
Q9CR68	Cytochrome b-c1 complex subunit Rieske, mitochondrial	46.35	2.41E-02	7	−1.34
Q03265	ATP synthase subunit α, mitochondrial	54.97	1.74E-02	27	−1.33
P35486	Pyruvate dehydrogenase E1 component subunit α, somatic form, mitochondrial	19.74	1.04E-02	6	−1.31
Q9CZ13	Cytochrome b-c1 complex subunit 1, mitochondrial	19.17	1.58E-02	9	−1.31
P05202	Aspartate aminotransferase, mitochondrial	26.98	6.45E-03	10	−1.30
Q921G7	Electron transfer flavoprotein-ubiquinone oxidoreductase, mitochondrial	1.14	1.18E-02	1	−1.29
A2ASS6	Titin	19.75	2.43E-02	550	−1.29
Q8BWT1	3-ketoacyl-CoA thiolase, mitochondrial	25.19	9.29E-03	9	−1.28
P56382	ATP synthase subunit ϵ, mitochondrial	28.85	1.16E-02	2	−1.27

TABLE V

Overrepresented proteins in laminin α2 chain–deficient diaphragm versus wild-type diaphragm

Accession	Description	Σ Coverage	*p* value	Σ Number of peptides	Fold change
P13541	Myosin-3	23.09	2.54E-02	50	4.36
Q62009	Periostin	4.30	1.58E-03	2	3.93
P48678	Prelamin-A/C	26.32	2.18E-03	14	1.87
P51885	Lumican	25.15	2.35E-02	7	1.83
P62962	Profilin-1	27.14	5.01E-03	3	1.83
P16045	Galectin-1	17.78	4.82E-03	2	1.77
P13542	Myosin-8	48.89	6.58E-03	111	1.70
P10107	Annexin A1	10.40	5.55E-03	3	1.65
P19123	Troponin C, slow skeletal and cardiac muscles	23.60	2.21E-02	3	1.60
P68433	Histone H3.1	16.91	1.61E-02	3	1.58
P17742	Peptidyl-prolyl cis-trans isomerase A	27.44	1.71E-02	5	1.54
Q9DBJ1	Phosphoglycerate mutase 1	15.35	7.96E-03	4	1.52
P20152	Vimentin	53.86	5.22E-04	26	1.49
P43276	Histone H1.5	8.97	3.60E-03	2	1.48
P28653	Biglycan	28.18	1.45E-02	8	1.47
P48036	Annexin A5	22.88	7.78E-03	7	1.43
Q9D0J8	Parathymosin	11.88	2.75E-02	1	1.42
P15864	Histone H1.2	33.02	4.90E-03	9	1.41
P10854	Histone H2B type 1-M	47.62	9.23E-03	7	1.39
P14131	40S ribosomal protein S16	11.64	8.48E-03	2	1.34
P47963	60S ribosomal protein L13	2.84	2.48E-04	1	1.32
P43274	Histone H1.4	31.96	2.36E-02	8	1.31
P07356	Annexin A2	17.99	1.59E-02	6	1.31
P51881	ADP/ATP translocase 2	34.23	1.15E-03	11	1.27

DISCUSSION

Knowledge of the differences between normal and laminin α2 chain–deficient muscles is crucial for designing future treatment of MDC1A. Although several different approaches to combat muscular dystrophy in laminin α2 chain–deficient mouse models have been tested, and although these approaches include correction of both primary and secondary manifestations (11, 12, 25, 30, 41, 46–55), the clinical appliance is still years away. Thus, we performed a comparative proteomic analysis of dy^{3K}/dy^{3K} muscles, and we report an

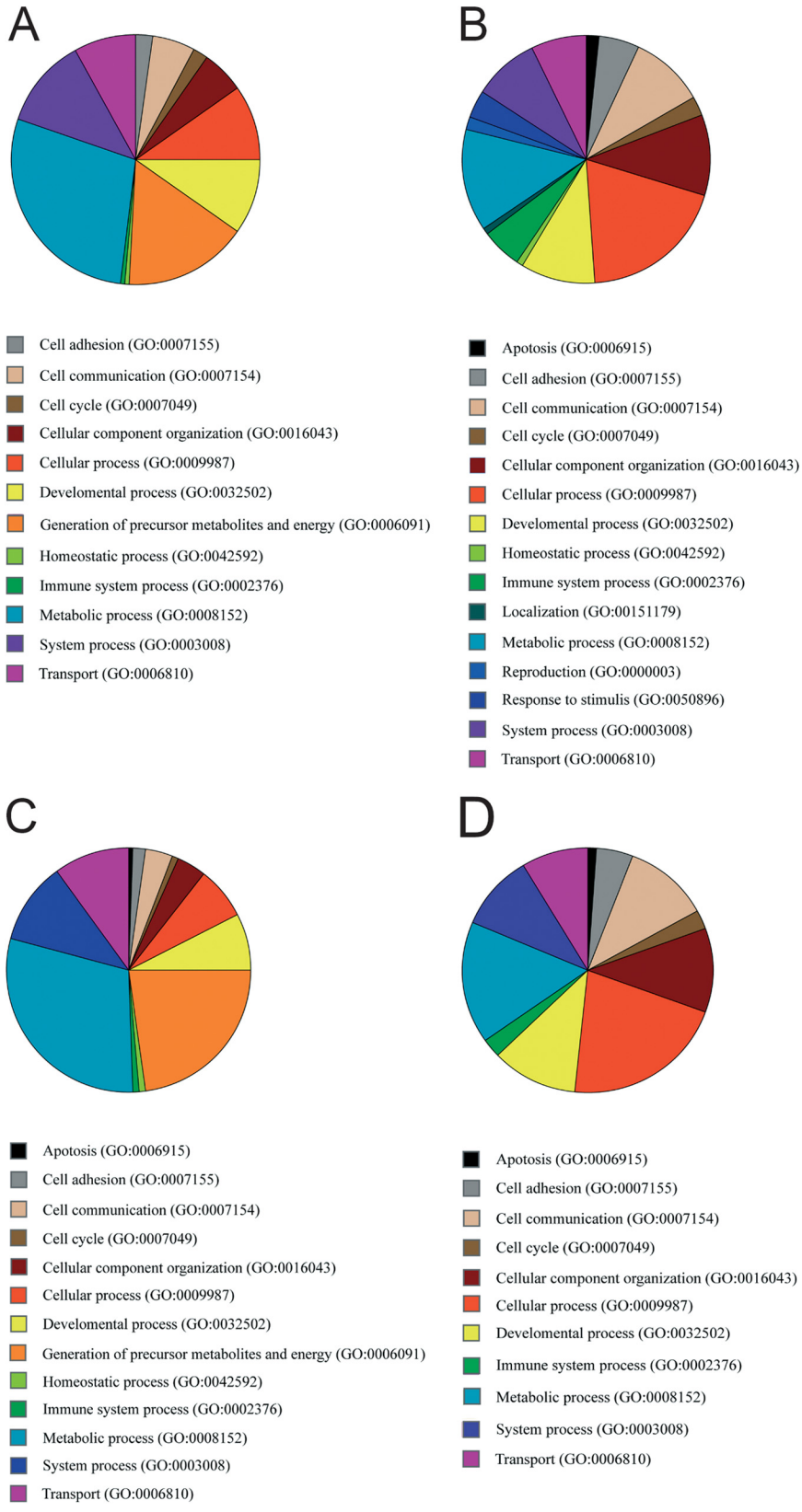

FIG. 1. **Pie charts of differentially expressed proteins in laminin α2 chain–deficient muscles grouped according to different biological processes using PANTHER classification.** *A*, down-regulated proteins in laminin α2 chain–deficient gastrocnemius. *B*, up-regulated proteins in laminin α2 chain–deficient gastrocnemius. *C*, down-regulated proteins in laminin α2 chain–deficient diaphragm. *D*, up-regulated proteins in laminin α2 chain–deficient diaphragm.

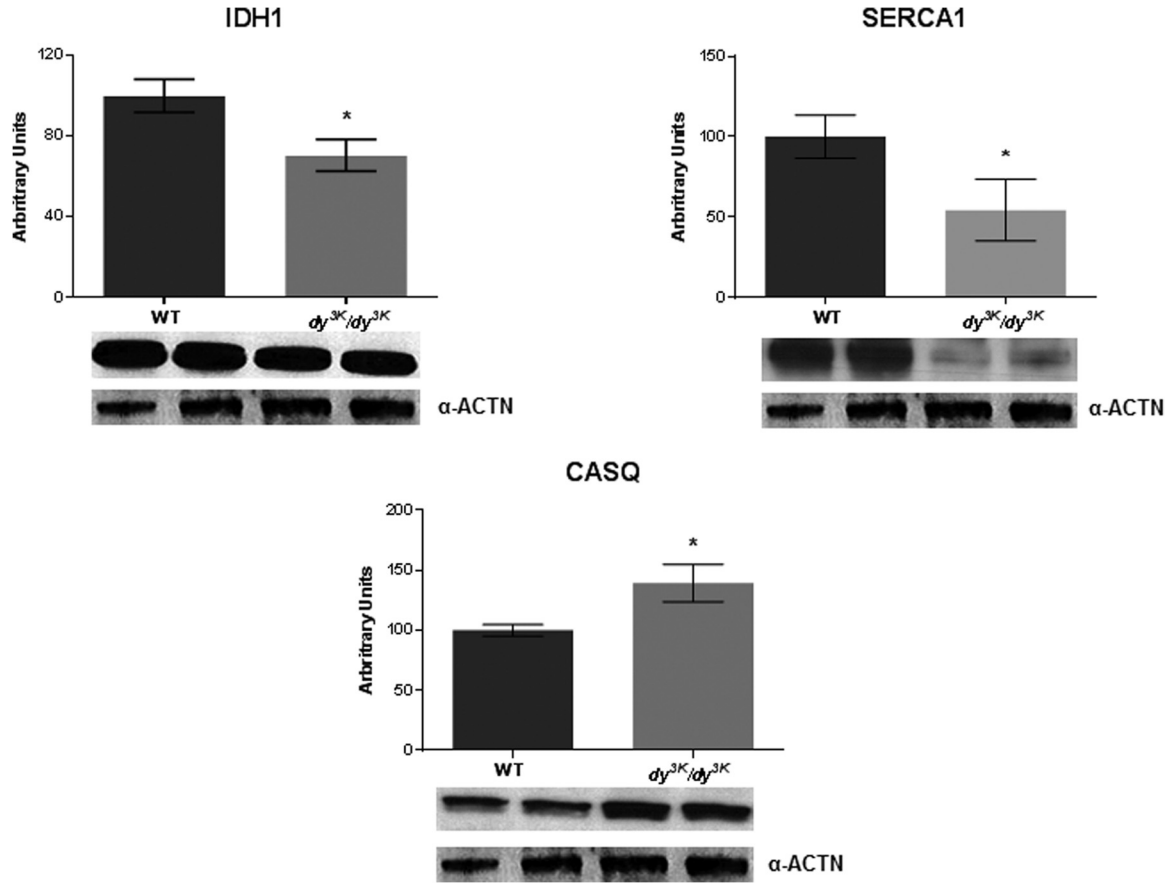

FIG. 2. **Western blot analysis of selected proteins.** Quantification of isocitrate dehydrogenase (IDH1), SERCA1, and calsequestrin (CASQ) by Western blot analysis of extracts of gastrocnemius muscle from wild-type and laminin $\alpha 2$ chain–deficient dy^{3K}/dy^{3K} mice. α-actinin (α-ACTN) was used as a loading control. $n = 4$ and $p < 0.05$, Mann–Whitney.

extensive catalogue of differentially expressed proteins in dystrophic muscle. A majority of the differentially expressed proteins are involved in metabolic processes (of which a majority take place in the mitochondria), calcium handling, or extracellular remodeling, making them valuable candidates for potential drug targets for MDC1A.

Similar metabolic crises and mitochondrial abnormalities have been reported in gene and/or proteome expression profiling of different types of muscular dystrophy, including Duchenne muscular dystrophy and sarcoglycanopathy (56, 57), and biochemical studies unveiled limitations in glycolytic and tricarboxylic acid cycle pathways and defective regulation of energy metabolism in *mdx* mice (58, 59). Also, metabolic defects in β-sarcoglycan-deficient mice have been reported (60). Thus, the metabolic crisis and mitochondrial abnormalities most likely represent secondary effects of laminin $\alpha 2$ chain deficiency and of muscular dystrophy in general, but we cannot entirely rule out that these are unique features of MDC1A. It will be important to investigate whether metabolic alterations are present before the dystrophic pathology becomes visible and/or in myoblasts that generally are not affected by disease. For example, energy metabolism was shown to be affected in *mdx* myoblasts (61). Despite prevalent metabolic alterations in many muscular dystrophies, it is interesting to note that only few attempts to restore energy metabolism have been made (62), and future efforts should therefore be considered.

We further showed that the expression of several calcium-binding proteins was altered in laminin $\alpha 2$ chain–deficient muscles, indicating their role as well as a role for calcium in disease pathology. In line with the hypothesis that calcium dysregulation could be a primary event in the onset of muscular dystrophy, several treatment approaches aimed at normalizing the calcium homeostasis in dystrophic muscle have been evaluated in mice, and in particular in the *mdx* mouse model for Duchenne muscular dystrophy (63–65). Notably, it has been demonstrated that overexpression of SERCA1 is beneficial in the *mdx* mouse, as well as in a mouse model for sarcoglycanopathy (65). However, whether SERCA1 overexpression attenuates laminin $\alpha 2$ chain–deficient muscular dystrophy remains to be demonstrated. Ablation of cyclophilin D encoding gene (which prevents mitochondrial calcium overload) reduced muscular dystrophy in *mdx* and sarcoglycan-deficient mice, as well as in laminin $\alpha 2$ chain–deficient animals, but whether pharmacological inhibition of cyclophilin diminishes pathology in laminin $\alpha 2$ chain–deficient animals

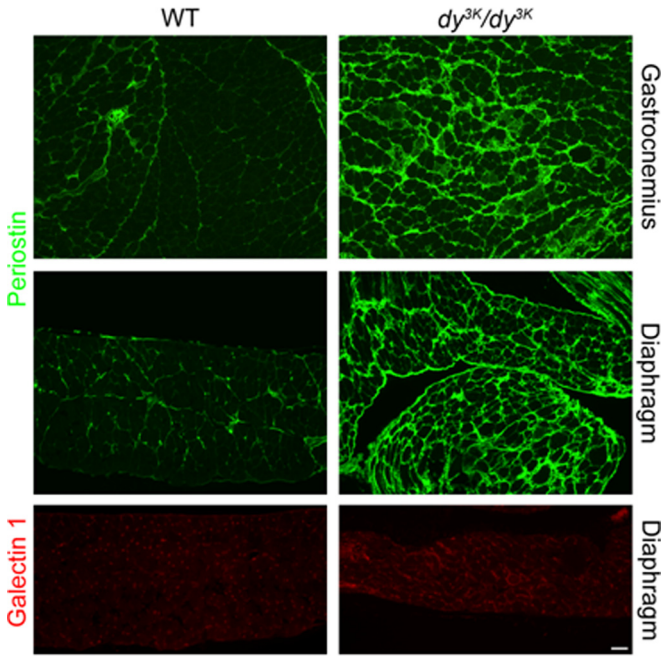

FIG. 3. **Periostin and galectin-1 are up-regulated in laminin α2 chain–deficient muscle.** Cross-sections of gastrocnemius and diaphragm muscles were stained with antibodies against periostin and galectin-1. Bar, 50 μm.

(like in *mdx* and sarcoglycan-deficient mice) is not known (37). Thus, further approaches aimed at modulating calcium regulation in laminin α2 chain–deficient muscles should be tested.

Finally, it was recently demonstrated that anti-fibrotic therapy is beneficial in mouse models for MDC1A. Losartan and an analog derivative inhibited TGF-β signaling and reduced fibrosis and inflammation in skeletal muscle of two different mouse models (54, 55). Yet, TGF-β1 has a very broad spectrum of action. Therefore, it becomes important to elucidate the composition of the inflammatory/fibrotic tissue in laminin α2 chain–deficient muscle in more detail, as such exhaustive information might be helpful for the design of more specific anti-fibrotic treatments. For example, the expression of periostin, which has been suggested to function upstream but also downstream of TGF-β (66), was significantly increased in laminin α2 chain–deficient muscles. Thus, it is tempting to speculate that the removal of periostin would reduce the pathogenesis of laminin α2 chain–deficient muscular dystrophy by decreasing fibrosis, just like the deletion of periostin significantly improved sarcoglycan-deficient muscle structure and function (67).

In summary, we have here mapped alterations in the proteomic signature of laminin α2 chain–deficient mouse muscle. Although we used a powerful tandem mass spectrometry methodology with TMT isobaric labels, it also has its weaknesses, including the problem of ratio distortion, and we acknowledge that the expression ratio changes might have been underestimated (68, 69). Nevertheless, we identified differences in around 100 proteins, and a major part of these proteins are involved in metabolic, calcium, and extracellular matrix homeostasis, indicating that these processes could be targets for MDC1A therapy.

Acknowledgments—We gratefully acknowledge SCIBLU Proteomics Resource Centre at Lund University (especially Karin Hansson) and the Proteomics Core Facility at Gothenburg University (in particular Carina Sihlbom) for excellent help with protein analysis. We also acknowledge the PRIDE team (Attilla Csordas) for the deposition of our data to the ProteomeXchange Consortium. The MS data have been deposited to the ProteomeXchange Consortium (http://proteomecentral.proteomexchange.org) via the PRIDE partner repository with the dataset identifier PXD000978. To access the data, please visit http://tinyurl.com/ojhrmot with username reviewer64343@ebi.ac.uk and password P07IsY9k.

* This work was supported by the Swedish Research Council. C.Y.M. was the recipient of a fellowship from CAPES (Grant No. 2014–10^{-6}). The instrument at the Proteomics Core Facility at Gothenburg University was funded by the Knut and Alice Wallenberg Foundation (Grant No. KAW2007.0118 to Gunnar C. Hanson).

S This article contains supplemental material.

** To whom correspondence should be addressed: Madeleine Durbeej, Department of Experimental Medical Science, Unit of Muscle Biology, Lund University, BMC B12, 221 84 Lund, Sweden, Tel.: 0046-46-2220812, Fax: 0046-46-2220855, E-mail: madeleine.durbeej-hjalt@med.lu.se.

‡ These authors contributed to this work equally.

REFERENCES

1. Allamand, V., and Guicheney, P. (2002) Merosin-deficient muscular dystrophy, autosomal recessive (MDC1A, MIM#156225, LAMA2 gene coding for α2 chain of laminin). *Eur. J. Hum. Genet.* **10,** 91–94
2. Helbling-Leclerc, A., Zhang, X., Topaloglu, H., Cruaud, C., Tesson, F., Weissenbach, J., Tomé, F. M. S., Schwartz, K., Fardeau, M., Tryggvason, K., and Guicheney, P. (1995) Mutations in the laminin α2 chain gene (LAMA2) cause merosin-deficient muscular dystrophy. *Nat. Genet.* **11,** 216–218
3. Voit, T., and Tomé, F. S. (2004) The congenital muscular dystrophies. In *Myology* (Angel, A., and Franzini-Armstrong, C., eds) Vol. 2, pp. 1203–1238, McGraw-Hill, New York
4. Ibraghimov-Beskrovnaya, O., Ervasti, J. M., Leveille, C. J., Slaughter, C. A., Sernett, S. W., and Campbell, K. P. (1992) Primary structure of dystrophin-associated glycoproteins linking dystrophin to the extracellular matrix. *Nature* **355,** 696–702
5. Talts, J. F., Andac, Z., Gohring, W., Brancaccio, A., and Timpl, R. (1999) Binding of the G domains of laminin α1 and α2 chains and perlecan to heparin, sulfatides, α-dystroglycan and several extracellular matrix proteins. *EMBO J.* **18,** 863–870
6. von der Mark, H., Williams, I., Wendler, O., Sorokin, L., von der Mark, K., and Pöschl, E. (2002) Alternative splice variants of α7β1 integrin selectively recognize different laminin isoforms. *J. Biol. Chem.* **277,** 6012–6016
7. Gawlik, K. I., and Durbeej, M. (2011) Skeletal muscle laminin and MDC1A: pathogenesis and treatment strategies. *Skelet. Muscle* **1,** 9
8. Han, R., Kanagawa, M., Yoshida-Moriguchi, T., Rader, E. P., Ng, R. A., Michele, D. E., Muirhead, D. E., Kunz, S., Moore, S. A., Iannaccone, S. T., Miyake, K., McNeil, P. L., Mayer, U., Oldstone, M. B. A., Faulkner, J. A., and Campbell, K. P. (2009) Basal lamina strengthens cell membrane integrity via the laminin G domain-binding motif of α-dystroglycan. *Proc. Natl. Acad. Sci. U.S.A.* **106,** 12573–12579
9. Vachon, P. H., Xu, H., Liu, L., Loechel, F., Hayashi, Y., Arahata, K., Reed, J. C., Wewer, U. M., and Engvall, E. (1997) Integrins (α7β1) in muscle function and survival. Disrupted expression in merosin-deficient congenital muscular dystrophy. *J. Clin. Invest.* **10,** 1870–1881
10. Mayer, U. (2003) Integrins: redundant or important players in skeletal muscle and beyond. *J. Biol. Chem.* **279,** 14587–14590
11. Gawlik, K. I., Mayer, U., Blomberg, K., Sonnenberg, A., Ekblom, P., and

Durbeej, M. (2006) Laminin α1 chain mediated reduction of laminin α2 chain deficient muscular dystrophy involves integrin $\alpha7\beta1$ and dystroglycan. *FEBS Lett.* **580,** 1759–1765
12. Moll, J., Barzaghi, P., Lin, S., Bezakova, G., Lochmuller, H., Engvall, E., Muller, U., and Ruegg, M. A. (2001) An agrin minigene rescues dystrophic symptoms in a mouse model for congenital muscular dystrophy. *Nature* **413,** 302–307
13. Doran, P., Martin, G., Dowling, P., Jockusch, H., and Ohlendieck, K. (2006) Proteome analysis of the dystrophin-deficient MDX diaphragm reveals a drastic increase in the heat shock protein cvHSP. *Proteomics* **6,** 4610–4621
14. Gardan-Salmon, D., Dixon, J. M., Lonergan, S. M., and Selsby, J. T. (2011) Proteomic assessment of the acute phase of dystrophin deficiency in mdx mice. *Eur. J. Appl. Physiol.* **111,** 2763–2773
15. Carberry, S., Zweyer, M., Swandulla, D., and Ohlendieck, K. (2012) Proteomics reveals drastic increase of extracellular matrix proteins collagen and dermatopontin in the aged mdx diaphragm model of Duchenne muscular dystrophy. *Int. J. Mol. Med.* **30,** 229–234
16. Ge, Y., Molloy, M. P., Chamberlain, J. S., and Andrews, P. C. (2003) Proteomic analysis of mdx skeletal muscle: great reduction of adenylate kinase 1 expression and enzymatic activity. *Proteomics* **3,** 1895–1903
17. Guevel, L., Lavoie, J. R., Perez-Iratxeta, C., Rouger, K., Dubreil, L., Feron, M., Talon, S., Brand, M., and Megeney, L. A. (2010) Quantitative proteomic analysis of dystrophic dog muscle. *J. Proteome Res.* **10,** 2465–2449
18. Matsumura, C. Y., Menezes de Oliveira, B., Durbeej, M., and Marques, M. J. (2013) Isobaric tagging-based quantification for proteomic analysis: a comparative study of spared and affected muscles from mdx mice at the early phase of dystrophy. *PLoS One* **8,** e65831
19. Rayavarapu, S., Coley, W., Cakir, E., Jahnke, V., Takeda, S., Aoki, Y., Grodish-Dressman, H., Jaiswal, J. K., Hoffman, E. P., Brown, K. J., Hathout, Y., and Nagaraju, K. (2013) Identification of disease specific pathways using *in vivo* SILAC proteomics in dystrophin deficient *mdx* mouse. *Mol. Cell. Proteomics* **12,** 1061–1073
20. Lewis, C., Carverry, S., and Ohlendieck, K. (2009) Proteomic profiling of x-linked muscular dystrophy. *J. Muscle Res. Cell. Motil.* **30,** 267–279
21. De la Torre, C., Illa, I., Faulkner, G., Soria, L., Robles-Cedeno, R., Pereles-Dominguez-Perles, R., De Luna, N., and Gallardo, E. (2009) Proteomics identification of differentially expressed proteins in the muscle of dysferlin myopathy patients. *Proteomics Clin. Appl.* **3,** 486–497
22. de Morrée, A., Hensbergen, P. J., van Haagen, H. H., Dragan, I., Deelder, A. M., 't Hoen, P. A., Frants, R. R., and van der Maarel, S. M. (2010) Proteomic analysis of the dysferlin protein complex unveils its importance for sarcolemmal maintenance and integrity. *PLoS One* **5,** e13854
23. Washburn, M., Wolters, D., and Yates, J., III (2001) Large scale analysis of the yeast proteome by multidimensional protein identification technology. *Nat. Biotechnol.* **19,** 242–247
24. Thompson, A., Schäfer, J., Kuhn, K., Kienle, S., Schwarz, J., Schmidt, G., Neumann, T., Johnstone, R., Mohammed, A. K., and Hamon, C. (2003) Tandem mass tags: a novel quantification strategy for comparative analysis of complex protein mixtures by MS/MS. *Anal. Chem.* **75,** 1895–904
25. Carmignac, V., Quere, R., and Durbeej, M. (2011) Proteasome inhibition improves the muscle of laminin α2 chain-deficient mice. *Hum. Mol. Genet.* **20,** 541–552
26. Vizcaíno, J. A., Deutsch, E. W., Wang, R., Csordas, A., Reisinger, F., Ríos, D., Dianes, J. A., Sun, Z., Farrah, T., Bandeira, N., Binz, P. A., Xenarios, I., Eisenacher, M., Mayer, G., Gatto, L., Campos, A., Chalkley, R. J., Kraus, H. J., Albar, J. P., Martinez-Bartolomé, S., Apweiler, R., Omenn, G. S., Martens, L., Jones, A. R., and Hermjakob, H. (2014) ProteomeXchange provides globally co-ordinated proteomics data submission and dissemination. *Nat. Biotechnol.* **32,** 223–226
27. Karp, N. A., McCormick, P. S., Russell, M. R., and Lilley, K. S. (2007) Experimental and statistical considerations to avoid false conclusions in proteomics studies using differential in-gel electrophoresis. *Mol. Cell. Proteomics* **6,** 1354–1364
28. Storey, J. D., and Tibshirani, R. (2003) Statistical significance for genome wide studies. *Proc. Natl. Acad. Sci. U.S.A.* **100,** 9440–9445
29. Levin, Y. (2011) The role of statistical power analysis in quantitative proteomics. *Proteomics* **11,** 2565–2567
30. Gawlik, K., Miyagoe-Suzuki, Y., Ekblom, P., Takeda, S., and Durbeej, M. (2004) Laminin α1 chain reduces muscular dystrophy in laminin α2 chain deficient mice. *Hum. Mol. Genet.* **13,** 1775–1784
31. Kline, K. G., and Wu, C. C. (2009) MudPIT analysis: application to human heart tissue. *Methods Mol. Biol.* **528,** 281–293
32. Martins de Souza, D., Oliveira, B. M., Castro-Dias, E., Winck, F. V., Horiuchi, R. S., Baldasso, P. A., Caetano, H. T., Pires, N. K., Marangoni, S., and Novello, J. C. (2008) The untiring search for the most complete proteome representation: reviewing the methods. *Brief Funct. Genomic. Proteomic.* **7,** 312–321
33. Miyagoe, Y., Hanaoka, K., Nonaka, I., Hayasaka, M., Nabeshima, Y., Arahata, K., Nabeshima, Y., and Takeda, S. (1997) Laminin α2 chain-null mutant mice by targeted disruption of the Lama2 gene: a new model of merosin (laminin 2)-deficient congenital muscular dystrophy. *FEBS Lett.* **415,** 33–39
34. Häger, M., Bigotti, M. G., Meszaros, R., Carmignac, V., Holmberg, J., Allamand, V., Åkerlund, M., Kalamajski, S., Brancaccio, A., Mayer, U., and Durbeej, M. (2008) Cib2 binds integrin $\alpha7B\beta1D$ and is reduced in laminin α2 chain-deficient muscular dystrophy. *J. Biol. Chem.* **283,** 24760–247695
35. Deconinck, N., and Dan, B. (2007) Pathophysiology of Duchenne muscular dystrophy: current hypotheses. *Pediatr. Neurol.* **26,** 1–7
36. Vandebrouck, C., Martin, D., Colson-Van Schoor, M., Debaix, H., and Gailly, P. (2002) Involvement of TRPC in the abnormal calcium influx observed in dystrophic (mdx) mouse skeletal muscle fibers. *J. Cell Biol.* **158,** 1089–1096
37. Millay, D. P., Sargent, M. A., Osinska, H., Baines, C. P., Barton, E. R., Vuagniaux, G., Sweeney, H. L., Robbins, J., and Molkentin, J. D. (2008) Genetic and pharmacologic inhibition of mitochondrial-dependent necrosis attenuates muscular dystrophy. *Nat. Med.* **14,** 442–447
38. Millay, D. P., Goonasekera, S. A., Sargent, M. A., Maillet, M., Aronow, B. J., and Molkentin, J. D. (2009) Calcium influx is sufficient to induce muscular dystrophy through a TRPC-dependent mechanism. *Proc. Natl. Acad. Sci. U.S.A.* **106,** 19023–19028
39. Culligan, K. G., and Ohlendieck, K. (2002) Abnormal calcium handling in muscular dystrophy. *Basic Appl. Myol.* **12,** 147–157
40. Straub, V., Rafael, J. A., Chamberlain, J. S., and Campbell, K. P. (1997) Animal models for muscular dystrophy show different patterns of sarcolemmal disruption. *J. Cell Biol.* **139,** 375–385
41. Gawlik, K. I., Åkerlund, M., Carmignac, V., Elamaa, H., and Durbeej, M. (2010) Distinct roles for laminin globular domains in laminin α1 chain mediated rescue of murine laminin α2 chain deficiency. *PLoS One* **5,** e11549
42. Rescher, U., and Gereke, V. (2004) Annexins—unique membrane binding proteins with diverse functions. *J. Cell Sci.* **117,** 2631–2639
43. Probst-Cousinm, S., Berghoff, C., Neundörfer, B., and Heuss, D. (2004) Annexin expression in inflammatory myopathies. *Muscle Nerve* **30,** 102–110
44. Jeudi, S., Wardrop, K. E., Alessi, A., and Dominov, J. A. (2011) Bcl-2 inhibits the innate immune response during early pathogenesis of murine congenital muscular dystrophy. *PLoS One* **6,** e22369
45. Taniguchi, M., Kurahashi, H., Noguchi, S., Sese, J., Okinaga, T., Tsukahara, T., Guicheney, P., Ozono, K., Nishino, I., Morishita, S., and Toda, T. (2006) Expression profiling from Fukuyama-type congenital muscular dystrophy and laminin-α2 deficient congenital muscular dystrophy; is congenital muscular dystrophy a primary fibrotic disease? *Biochem. Biophys. Res. Commun.* **342,** 489–502
46. Kuang, W., Xu, H., Vachon, P. H., and Engvall, E. (1998) Merosin-deficient congenital muscular dystrophy. Partial genetic correction in two mouse models. *J. Clin. Invest.* **102,** 844–852
47. Meinen, S., Barzaghi, P., Lin, S., Lochmuller, H., and Rüegg M. A. (2007) Linker molecules between laminins and dystroglycan ameliorate laminin-α2-deficient muscular dystrophy at all disease stages. *J. Cell Biol.* **176,** 979–993
48. Doe, J. A., Wuebbles, R. D., Allred, E. T., Rooney, J. E., Elorza, M., and Burkin, D. J. (2011) Transgenic overexpression of the α7 integrin reduces muscle pathology and improves viability in the dy(W) mouse model of merosin-deficient congenital muscular dystrophy type 1A. *J. Cell Sci.* **124,** 2287–2297
49. Girgenrath, M., Dominov, J. A., Kostek, C. A., and Miller, J. B. (2004) Inhibition of apoptosis improves outcome in a model of congenital muscular dystrophy. *J. Clin. Invest.* **114,** 1635–1639
50. Erb, M., Meinen, S., Barzaghi, P., Sumanovski, L. T., Courdier-Fruh, I.,

Rüegg, M. A., and Meier, T. (2009) Omigapil ameliorates the pathology of muscle dystrophy caused by laminin-α2 deficiency. *J. Pharmacol. Exp. Ther.* **331,** 787–795
51. Kumar, A., Yamauchi, J., Girgenrath, T., and Girgenrath, M. (2011) Muscle-specific expression of insulin-like growth factor 1 improves outcome in Lama2Dy-w mice, a model for congenital muscular dystrophy type 1A. *Hum. Mol. Genet.* **20,** 2333–2343
52. Carmignac, V., Svensson, M., Körner, Z., Elowsson, L., Matsumura, C., Gawlik, K., Allamand, V., and Durbeej, M. (2011) Autophagy is increased in laminin α2 chain-deficient muscle and inhibition improves muscle morphology in a mouse model of MDC1A. *Hum. Mol. Genet.* **20,** 4891–4902
53. Rooney, J. E., Knapp, J. R., Hodges, B. L., Wuebbles, R. D., and Burkin, D. J. (2011) Laminin-111 protein therapy reduces muscle pathology and improves viability of a mouse model of merosin-deficient congenital muscular dystrophy. *Am. J. Pathol.* **180,** 1593–1602
54. Elbaz, M., Yanay, N., Aga-Mizrachi, S., Brunschwig, Z., Kassis, I., Ettinger, K., Barak, V., and Nevo, Y. (2012) Losartan, a therapeutic candidate in congenital muscular dystrophy: Studies in the dy^{2J}/dy^{2J} mouse. *Ann. Neurol.* **71,** 699–708
55. Meinen, S., Lin, S., and Rüegg, M. A. (2012) Angiotensin II type 1 receptor antagonists alleviate muscle pathology in the mouse model for laminin-α2-deficient congenital muscular dystrophy (MDC1A). *Skelet. Muscle* **2,** 18
56. Turk, R., Sterrenburg, E., van der Wees, C. G., de Meijer, E. J., de Menezes, R. X., Groh, S., Campbell, K. P., Noguchi, S., van Ommen, G. J., den Dunnen, J. T., and 't Hoen, P. A. (2006) Common pathological mechanisms in mouse models for muscular dystrophies. *FASEB J.* **20,** 127–129
57. Chen, Y. W., Zhao, P., Borup, R., and Hoffman, E. P. (2000) Expression profiling in the muscular dystrophies: identification of novel aspects of molecular pathophysiology. *J. Cell Biol.* **151,** 1321–1336
58. Chinet, A. E., Even, P. C., and Decrouy, A. (1994) Dystrophin-dependent efficiency of metabolic pathways in mouse skeletal muscles. *Experientia* **59,** 602–605
59. Even, P. C., Decrouy, A., and Chinet, A. (1994) Defective regulation of energy metabolism in the mdx-mouse skeletal muscles. *Biochem. J.* **304,** 649–654
60. Groh, S., Zong, H., Goddeeris, M. M., Lebakken, C. S., Venzke, D., Pessin, J. E., and Campbell, K. P. (2009) Sarcoglycan complex: implications for metabolic defects in muscular dystrophies. *J. Biol. Chem.* **284,** 19178–19182
61. Onopiuk, M., Brutkowski, W., Wierzbicka, K., Wojciechowska, S., Szczepanowska, J., Fronk, J., Lochmuller, H., Gorecki, D. C., and Zablocki, K. (2009) *Biochem. Biophys. Res. Commun.* **386,** 463–466
62. Le Borgne, F., Guyot, S., Logerot, M., Beney, L., Gervais, P., and Demarquoy, J. (2012) Exploration of lipid metabolism in relation with plasma membrane properties of Duchenne muscular dystrophy cells: influence of L-carnitine. *PLoS One* **7,** e49346
63. Matsumura, C. Y., Pertille, A., Albuquerge, T. C., Santo Neto, H., and Marques, M. J. (2009) Diltiazem and verapamil protect dystrophin-deficient muscle fibers of MDX mice from degeneration: a potential role in calcium buffering and sarcolemmal stability. *Muscle Nerve* **39,** 167–176
64. Jørgensen, L. H., Blain, A., Greally, E., Lavala, S. H., Blamire, A. M., Davison, B. J., Brinkmeier, H., MacGowan, G. A., Schrøder, H. D., Bushby, K., Straub, V., and Lochmüller, H. (2011) Long-term blocking of calcium channels in mdx mice results in differential effects on heart and skeletal muscle. *Am. J. Pathol.* **178,** 273–283
65. Goonasekera, S. A., Lam, C. K., Millay, D. P., Sargent, M. A., Hajjar, R. J., Kranias, E. G., and Molkentin, J. D. (2011) Mitigation of muscular dystrophy in mice by SERCA overexpression in skeletal muscle. *J. Clin. Invest.* **121,** 1044–1052
66. Horiuchi, K., Amizuka, N., Takeshita, S., Takamatsu, H., Katsuura, M., Ozawa, H., Toyama, Y., Bonewald, L. F., and Kudo, A. (1999) Identification and characterization of a novel protein, periostin, with restricted expression to periosteum and periodontal ligament and increased expression by transforming growth factor β. *J. Bone Miner. Res.* **14,** 1239–1249
67. Lorts, A., Schwanekamp, J. A., Baudino, T. A., McNally, E. M., and Molkentin, J. D. (2012) Deletion of periostin reduces muscular dystrophy and fibrosis in mice by modulating the transforming growth factor-β pathway. *Proc. Natl. Acad. Sci. U.S.A.* **109,** 10978–10983
68. Ting, L., Rad, R., Gygi, S. P., and Haas, W. (2011) MS3 eliminates ratio distortion in isobaric multiplexed quantitative proteomics. *Nat. Methods* **8,** 937–940
69. Christoforou, A., and Lilley, K. S. (2011) Taming the isobaric tagging elephant in the rooms in quantitative proteomics. *Nat. Methods* **8,** 911–913